Photonic Crystal Analog to Digital Converter A Literature Review, Challenges, and Some Novel Trends

Tamer S. Mostafa[1],AmanyM.Ahmed[2],andEl- Sayed M. El- Rabaie[3]
[1]Department of Telecommunication, Faculty of Engineering, Egyptian Russian University, Cairo, Egypt, P.O. 11829, (algwaal@yahoo.com). Orcid: **0000-0001-6100-7466**
[2]Department of Telecommunication, Giza Engineering institute, Giza, Egypt, P.O. 32952, (eng.amany35@gmail.com).
[3]Department of Electronics and Electrical Communications Engineering, Faculty of Electronic Engineering, Menoufia University, Menouf, Egypt, P.O. 32952, (elsayedelrabaie@gmail.com).

Abstract— This paper reviews all-optical analog to digital converters (OADCs) based on the photonic crystal. They are nonlinear applications and are used in all-optical data processing systems. They are consisting of one input (i.e., continuous analog optical signal) and two or five outputs (i.e., binary code). Most of these structures have two operation steps. The first one is a nonlinear demultiplexer followed by second stage that has an optical coder. The demultiplexer creates the discrete levels for the continuous optical input signal; then the optical coder generates output bits. There are two techniques to design OADC, ring and cavity resonators. All OADCs structures use the finite difference time domain (FDTD) and plane wave expansion (PWE) analysis methods. The paper presents a comparison between the different designs in the literature for both the ring and cavity resonators using the RSOFT simulator followed by the challenges and some novel trends.

Keywords— Photonic crystal, Optical ADC, ring resonator, Demultiplexer, Optical encoder.

Introduction

Photonic crystals (Ph. Cs.) are good choices to realize all optical components. Photonic crystals are appropriate for implementing optical communications systems, signal processing systems and optical integrated circuits [1]. Processing signals is an important stage in communication networks, it is recommended to have separate digital signals as inputs of the signal processing stage [2], so a conversion process is required to get discrete optical waves from analog ones. Therefore, OADCs are so important to realize the complete optical networks.

In all (OADC), nonlinear materials are essentials, so high input power is needed. The main disadvantages of using nonlinear materials are the narrow range of frequency and the difficulty of integration with optical devices that made of silicon. The nonlinear material is efficient use of data. Nonlinear regression can help us to make an estimate of unknown parameters of the model using small sets of data. Most of these structures have two operation steps. The first one is a nonlinear demultiplexer and followed by the second stage that has an optical coder. The demultiplexer creates the discrete levels for the continuous optical input signal; then the optical coder is generating output bits.

The OADC is a device that can convert analog signal to standard binary codes (zero, one) from the optical intensity of the input signal. It has been shown that the optical behavior of (Ph. Cs.) depends considerably on the refractive index of the material structure [3,4].The techniques are ring and cavity resonators to design OADC. The advantages of applying these techniques are decreasing footprint (i.e. total area of the ADC structure) to minimize the leakage loss and improve the maximum sampling rate.

The trend now is converting electronic devices to an optical integrated circuit to improve the bandwidth and the speed of operation. The drawbacks of electronic solutions are: big size, chip-scale integration, high-power consumption, low signal-to-noise ratio, low-speed and narrow operating wavelength bandwidth. We can solve these problems by using the (Ph. Cs.) technology [5]. Photonic crystal (ADC) improves the performance of sampling bit rate [6], transmission efficiency [7], speed and band width compared with electronic component. Moreover, its footprint is decreasing to micro and nano scales. It has low power consumption by using ring resonator [8, 9], cavity that are constructed by nonlinear materials. Many applications are made by using optical circuits, for examples optical filters [10– 23], demultiplexers [24–31], switches [32–36], logic gates [37– 47], sensors [48, 50], lasers [51], power splitter [52], encoder [53, 54], routers [55, 56], amplifiers [57- 61], memories [62, 63], couplers [64]. All nonlinear optical structures have low absorption coefficients and fast response times (i.e. picoseconds).

This paper provides in-depth survey for (OADC) based on (Ph. Cs.). An intensive review has been done on the (1x2), (1x4) and (1x5) dimensions. The classification of this study depends on ring and cavity resonators techniques. All the calculations and simulations of the proposed designs have been done using plane wave expansion (PWE) which is used as a numerical method to calculate the photonic band gap and finite-difference time domain (FDTD) [65]. These methods are applied to analyze propagation of electromagnetic wave. A concise elaboration was provided followed by comparison tables.

The remainder of this paper is organized as follows. The operating design techniques, analysis and simulation methods are provided in section 2. In section 3, a

discussion about the conventional analog to digital converters is given. A survey on the photonic crystal analog to digital converter based on ring resonator with two, four and five outputs followed by cavity resonator are provided in section 4 and 5, respectively. The challenges and some novel trends for the design of such devices were presented in section 6. The conclusion is introduced in section 7 followed by the more relevant reference.

I. Operating Design Techniques, Analysis and Simulation Methods

The two-dimensional (Ph. Cs.) platform is common in all the proposed structures. Different lattice types (i.e., square and Hexagonal) are used in the pillar scheme (i.e. rod on a background of air) to implement them. ADCs are built with line defect technique which is used in wave guide structure. Cavity and ring resonators techniques are used to improve the results. The resonant wavelength is determined based on the used resonance elements [66]. The change in refractive rod index and the input power can affect also on the resonant wavelength. According to the final design, the operating range of the wavelength will be determined.

A. The Photonic Band Gap

Photonic band gap (PBG) is the range of wavelengths where the light beam cannot propagate [67]. There are two methods of analyzing the (Ph. Cs.). These methods are Plane wave expansion (PWE) and finite difference time domain (FDTD). They are periodic structures, so (PWE) expresses the Eigen modes as a superposition of plane waves. Therefore, an accurate solution has been provided for the calculation of (PBG). The reason of the accurate calculation is the treat of just propagation modes [68]. Figure.1 shows the photonic band diagram representation of the fundamental transverse electric (TE) and transverse magnetic (TM) modes in (Ph. Cs.).

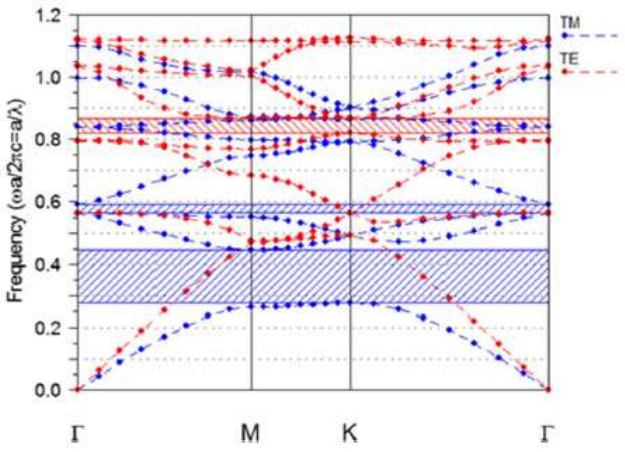

Fig.1 The photonic band diagram in photonic crystal [67].

(Ph. Cs.) is used for calculating the field distribution and transmission spectra and solving Maxwell's equations [69, 70]. The time-dependent representation for these equations can be shown as:

$$\frac{\partial \boldsymbol{H}}{\partial t} = -\frac{1}{\mu_r}\nabla \times \boldsymbol{E} \quad (1)$$

$$\frac{\partial \boldsymbol{E}}{\partial t} = -\frac{1}{\varepsilon_r}\nabla \times \boldsymbol{H} - \frac{\sigma_r}{\varepsilon_r}\boldsymbol{E} \quad (2)$$

where ε_r, μ_r, and σ_r are the spatial dependent permittivity, permeability, and conductivity of the material, respectively [71]. The E is the electric field and H is the magnetic field. For all proposed designs, the Gaussian modulated continuous wave (GMCW) signal is used as an input.

The sampling rate is a relation between the number of samples and sampling time. Moreover, the delay time and the switching speed can be calculated from the time response curves. The delay time is the time taken to climb the output power from 0 to 10% of the steady-state output power [72, 73]. The switching speed is the reciprocal of the delay [74].

II. A Conventional Analog to Digital Converter

Conventional ADCs can be implemented as shown below. Figure (2) consists of two blocks; the first one is a sampling and quantizing block, while the other is binary encoder block.

In the first block, a nonlinear demultiplexer is used to perform the sampling-quantization process. The second block is used to verify the code via a binary encoder. The optical input signal will be quantized into separate levels; afterwards, two-bit binary numbers are generated for every level as outputs after passes throw the binary encoder block [75].

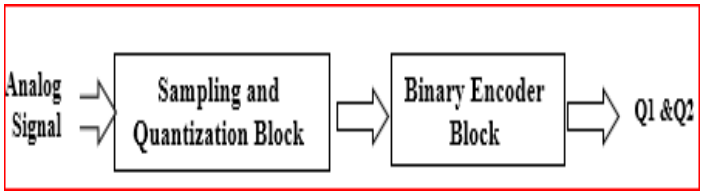

Fig.2 The block diagram of the conventional two-bit ADC [75].

The input optical analog signal is capable of generating standard binary codes in all (OADCs).

A. Numerical Method and Basic Structure

Analog to digital converters have a quantization block consists of only one input and multi levels output ports. In equation (3), the refractive index of nonlinear materials consists of linear refractive index (n_0) referred to

the usual, weak-field refractive index. The nonlinear refractive Index is (n_2) and (I) is the optical intensity of field. We can use equation (4) to obtain (n_2) and (I) [76]. (n_2) represents the rate at which the refractive index increases with increasing optical intensity [77].

$$n = n_o + n_2 I \tag{3}$$

$$I = 2n_o\varepsilon_o c|E(\omega)|^2 \tag{4}$$

The total polarization P due to second- and third-order nonlinearities is:

$$P = \varepsilon_o\left(x^{(1)}.\boldsymbol{E} + x^{(2)}:\boldsymbol{E^2} + x^{(3)} : \boldsymbol{E^3}\right) = P^{(1)} + P^{(2)} + P^{(3)} \tag{5}$$

Where $\chi^{(2)}$ (i.e. that can be neglected as considering the nonlinear material has crystal symmetries), $\chi^{(3)}$, and $\boldsymbol{E}$ are the second-order, third-order nonlinear susceptibilities, and the electric field [78], respectively. We considered that the nonlinear material has crystal symmetries, so The Kerr effect is:

$$n_2 = \frac{3\chi^3}{4n_o^2\varepsilon_o c} \tag{6}$$

Where c is the speed of light in space. The discrete levels in the presence of light with different power intensities can be generated by the nonlinear ring resonators located inside the waveguides [79].

III. Photonic Crystal Analog to Digital Converter Based on Ring Resonator

OADC is nonlinear application. That based on Kerr effect nonlinear coefficient in photonic crystal. In this section, the ring resonator technique is used to enhance the sampling rate. There are three types of ADC outputs, two, four and five bits.

A. Two Bit Optical Analog to Digital Converter (OADC)

A three ring resonators are used to implement 2-bits OADC [78] as shown in Fig.3. The design has a lattice constant (a) equal to 460 nm, PBG will be at 1390 nm <λ< 2010 nm, the refractive index n=2.78, radius of air holes r=0.3a, linear refractive index of n_0=1.5 and Kerr coefficient of n_2=10^{-16} m^2/W. Around 5% of normalized power back is reflected toward the input port. The total footprint is about 806 μm^2. The maximum sampling rate equals 200 GS/s.

As Mehdizadeh et al. reported in [79], the OADC block is consisting of a nonlinear triplexer and an optical coder. The triplexer has three hexagon ring resonator and it is used to generate discrete levels in the continuous input signal, and the optical coder converts the discrete levels coming from the triplexer to a 2-bit output. The structure has a=548 nm, n =3.46, n_0=1.4, n_2=10^{-14} m^2/W and r =0.185a as shown in Fig.4. It used a nonlinear material that made of doped glass.

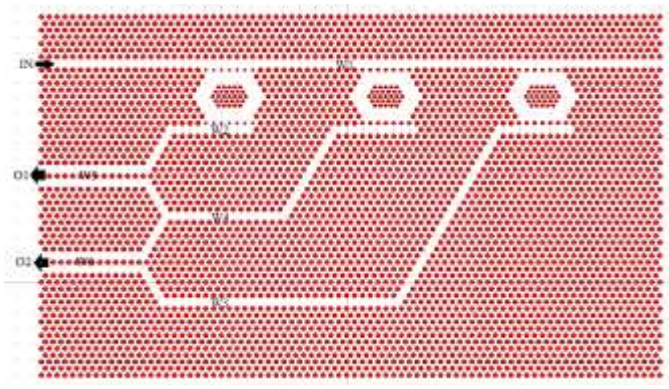

Fig.3 Two-bit with three ring resonator ADC [78].

The maximum delay time is achieved and equal to 5 ps. It has a large total footprint of 1520 μm^2 and the maximum sampling rate is around to 76.9 GS/s. These results are acceptable but not the best results according to all published works.

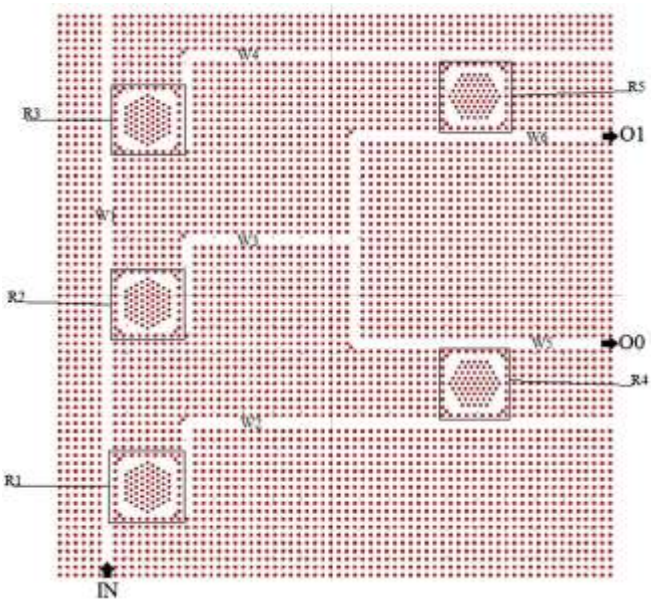

Fig.4 Triplexer and an optical coder of OADC [79].

This structure has a quantizer (i.e. demultiplexer) that has three nonlinear ring resonators to provide three discrete [80]. The nonlinear material is AlGaAs with n_2 =1.5 x 10^{-14} m^2/W and n_0 =1.4. A design has a= 570 nm and n_{si}=3.4 have been implemented in the air background. The main gain from this structure that it could able to reduce the loss and improve the transmission efficiency by use four ring resonators made of GaN. The PBG will be at 1360 nm <λ< 2040 nm with r=0.25a.

The structure of ring resonator ADC is illustrated in Fig.5, which has one input and two output ports. The maximum sampling rate will be about 220 GS/s with

footprint around 777.52 μm^2 and resolution sampling rate is 880 KS.

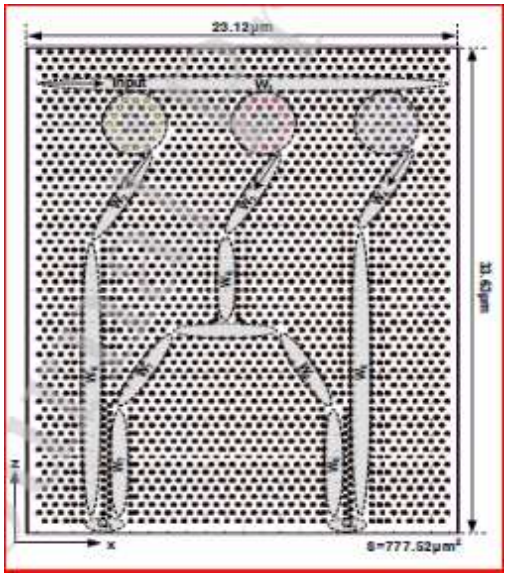

Fig.5 Optical ADC with three ring resonators [80].

As in [81], The structure of OADC has seven ring resonators. The lattice constant, radius of the Si rods and the refractive index are 595 nm,119 nm and 3.46 respectively as shown in Fig.6. The PBG is round at 1416 nm <λ< 2125 nm. Doped glass is the nonlinear rods in core section of the resonators. The nonlinear Kerr coefficient and the linear refractive index are 10^{-14} m^2/W and 1.4 for these rods. It has large footprint equal to 2016 μm^2 with maximum sampling rate equal to 250 GS/s. The fall times and the maximum rise are 0.5 ps and 1.5 ps, respectively.

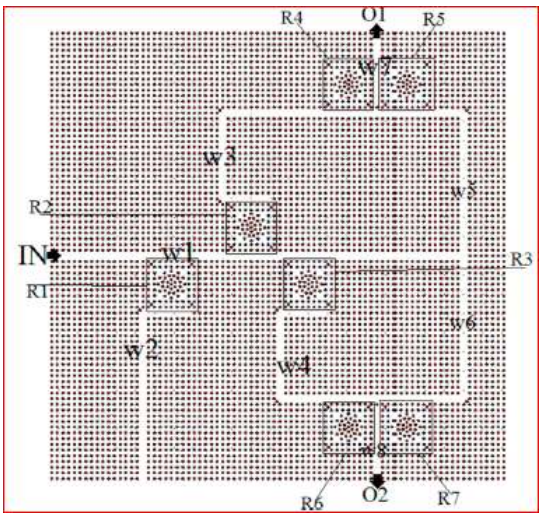

Fig.6 Optical ADC [81].

The (OADC) has two ring resonators and three nonlinear rods which are located inside the waveguide [82]. Two dimensions (Ph.Cs.) is made of linear material $Si_{0.75}Ge_{0.25}$ with n_{SiGe}=3.6 implemented in the air background and n_0 = 1.4. The structure has a= 570 nm and r=114 nm. the PBG will be at 1350 nm<λ< 1970 nm. Nonlinear part of structure has three rods whose nonlinear refractive is $n_2=10^{-17}$ m^2 /W.

At the output of the waveguide, there are green and blue nonlinearrods as shown in Fig.7. The behavior of optical field intensity can be controlled by the three nonlinear rods.

In this structure the sampling rate, footprint and resolution Sampling Rate are 300 GS/s, 240 μm^2 and 1200 KS, respectively. This structure has the best results as ADC compared with all other previous structures uses ring resonator technique.

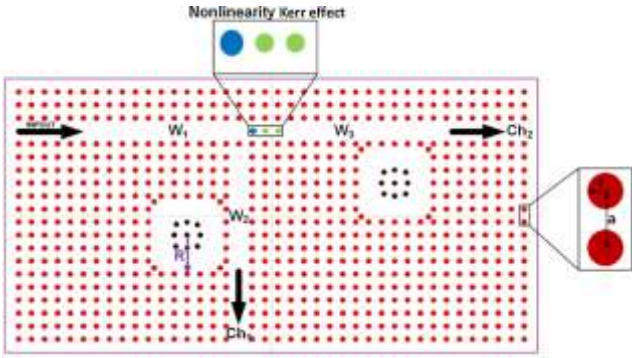

Fig.7 Two ring resonators and nonlinear rods ADC [82].

The ADC as in [83] based on nonlinear material made of doped glass. That has eight ring resonators as shown in Fig.8. The linear refractive index and Kerr coefficient are 1.4 and 10^{-14} m^2/W respectively. The maximum delay time is 4 ps.

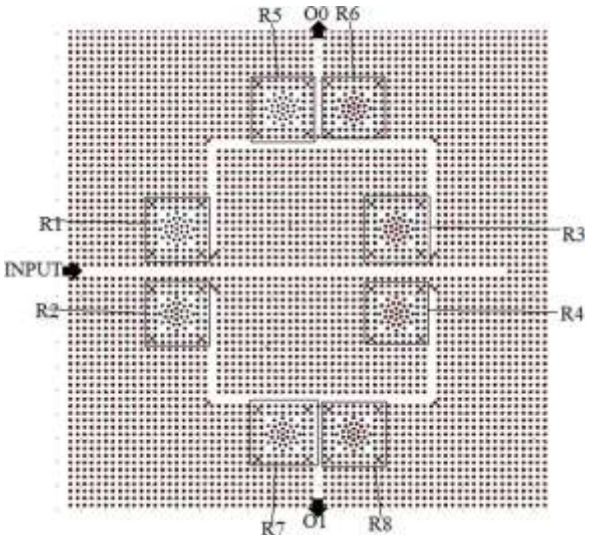

Fig.8 Two-bit ADC structure [83].

OADC using five nonlinear X-PCRRs with two-output bits. This structure contents of a three-channel demultiplexer [84]. As shown in Fig.9, a = 600 nm, R = 0.2a, n = 3.46 and the PBG in the wavelength range is 1333 nm <λ< 2142 nm. The nonlinear rods were made of doped glass whose n_0 = 1.4 and n_2= 10^{-14} m^2/W. The structure has five ring resonators and six waveguides. The maximum sampling rate is around 125GS/s, maximum time response of 4 ps, and the total footprint of 1785 μm^2. These results are suitable but not the best result.

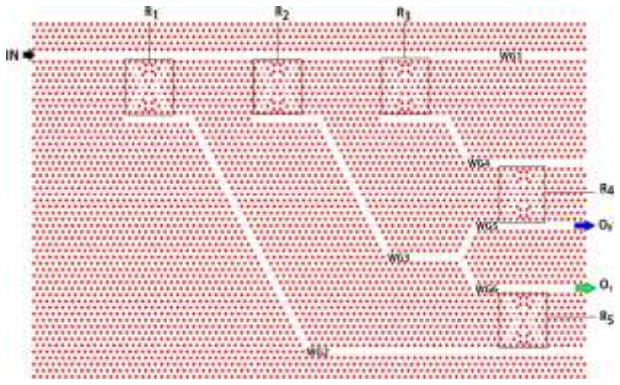

Fig.9 The schematic two-bit OADC [84].

We can do a brief comparison between all OADC in table1. It includes the most remarkable properties for each ring resonator design with one input and two output.

In [82], the results have been improved, the sampling rate of (OADC) is 300GS/s and footprint is 240 μm^2 when using two ring resonator and three nonlinear rode. The proposed structure gives good results compared to the previous results.

B. Four Bit Optical Analog to Digital Converter

ADC has one input and four outputs based on successive-like approximation. We use the Concept of successive-like approximation to quantize the signal into m bits of discrete levels; a regular coding system requires 2^m-1 discrete quantization levels [85]. So, this method discretes the input signal into only one quantized level [86, 87]. The threshold values are represented by x_i, i=1, 2, 3, 4 as shown in Fig.10.

The structure has octagon-like ring based on a square lattice (Ph. Cs.) in [88]. The structure has r=0.2a, a = 558 nm with relative permittivity of ϵ_r= n_0^2 = $(1.6)^2$, and relative permittivity of ϵ_b= n_b^2 = $(3.6)^2$ as shown in Fig.11. The nonlinear refractive index of Si-ncs's made by plasma-enhanced chemical vapor deposition (PECVD) is reported as n_2 = 10^{-16} m^2/W and n_0 = 1.5 and.

In [89], the octagonal-shape photonic crystal ring resonators (OSPCRRs) is representing bit of OADC. The structure has double rings of OSPCRRs (DR-OSPCRR). The lattice material $Si_{0.75}Ge_{0.25}$, a= 560 nm, r = 112 nm, and wavelength of band gap 1300 ≤λ ≤1880 nm as shown in Fig.12.

TABLE I. COMPARISONS BETWEEN THE PUBLISHED NONLINEAR ADC IN THE LITERATURE USING RING RESONATOR

Years	Wavelength 1550 nm	No. of wave guide	No. of ring resonator	Footprint (μm^2)	Lattice type	Lattice constant(a) nm	Refractive index	Linear refractive index	Nonlinear refractive index (m^2/w)	Radius of the Si rod (nm)	Input power range W/μm^2	Transfers (%)	Sampling Rate (GS/s)
[78, 2017]	1390< λ <2010	6	3	806	hexagon	460	2.78	1.5	10^{-16}	0.3a	0 - 0.016	60	200
[79, 2017]	1245< λ <1827	6	5	1520	square	548	3.46	1.4	10^{-14}	0.185a	0 - 0.1	75	76.9
[80, 2019]	1360< λ <2040	8	3	777.52	hexagonal	570	3.4	1.4	$1.5x10^{-17}$	0.2a	0- 4	65	220
[81, 2020]	1416< λ <2125	8	7	2016	square	595	3.46	1.4	10^{-14}	0.2a	0- 0.031	90	250
[82, 2020]	1350< λ <1970	3	2	240	square	570	3.6	1.4	10^{-17}	0.2a	0 - 10	89	300
[83, 2020]	NA	NA	8	NA	square	595	NA	1.4	10^{-14}	0.2a	0- 4	NA	NA
[84, 2021]	1333 < λ <2142	6	5	1785	hexagonal	600	3.46	1.4	10^{-14}	0.2a	0 - 2	95	125

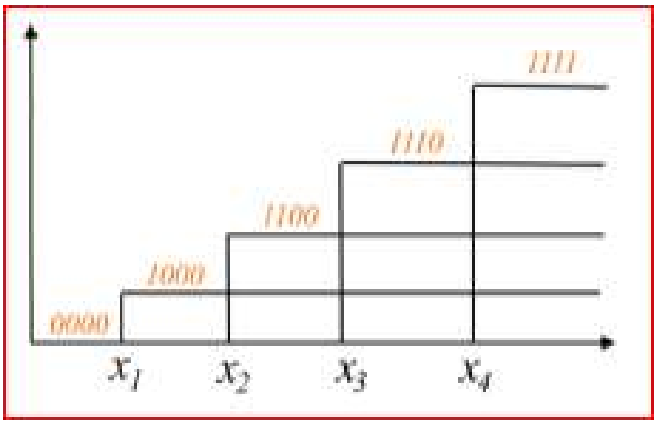

Fig.10 The coding system to represent ADC [85].

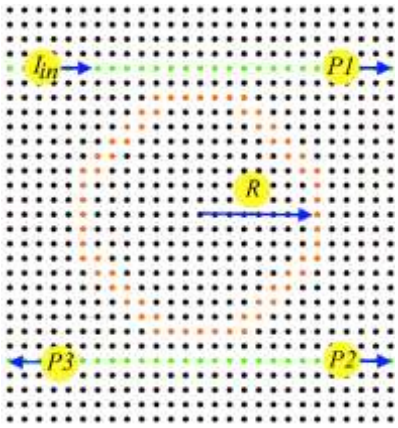

Fig.11 The single ring structure [88].

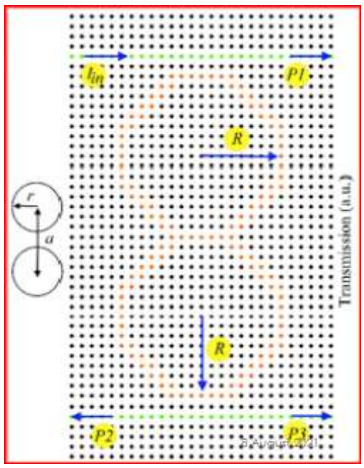

Fig.12 Two-vertical octagon-like rings [89].

C. *Five-Bit Optical Analog to Digital Converter*

In [90], A five-bit (AOADC) was created by cascading four optical limiters with different switching thresholds. The structure has two nonlinear (Ph. Cs.) ring resonators, the total foot print is about 1796 μm^2 and the bit rate is 500 GS/s. The design has a=587 nm, PBG will be at 1390, n=3.46, r=0.2a, and n_0=1.4. The nonlinear defects are made of doped glass, the nonlinear Kerr coefficient is 10^{-14} m^2/W shown in Fig. 13.

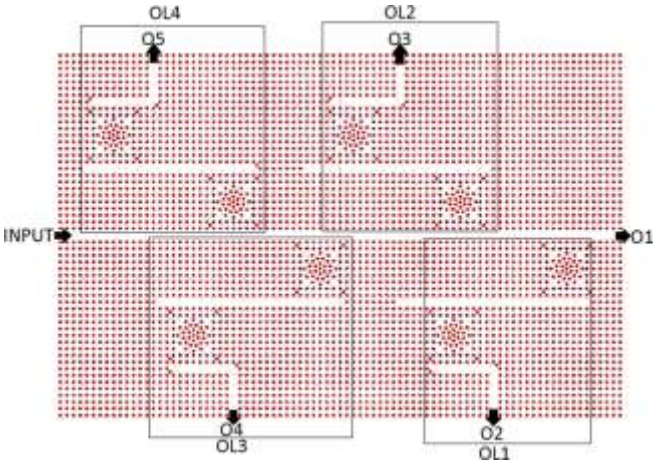

Fig. 13 Five-bit AOADC [90].

IV. PHOTOIC CRYSTAL ANALOG TO DIGITAL CONVERTER BASED ON RESONATE CAVITIES

The structure has a nonlinear 3-channel demultiplexer, followed by an optical coder [91]. The nonlinear demultiplexer consists of three nonlinear resonant cavities shown in Fig. 14. The structure has a = 725 nm, r =0.26a, n = 3.46 and The PBG region is equal to 1342 nm ≤ λ ≤1611 nm. One of the cavities can drop the optical beam to output port at suitable values of input signal optical intensity. The maximum sampling around to 52 GS/s and total footprint of the structure is about 924 μm^2.

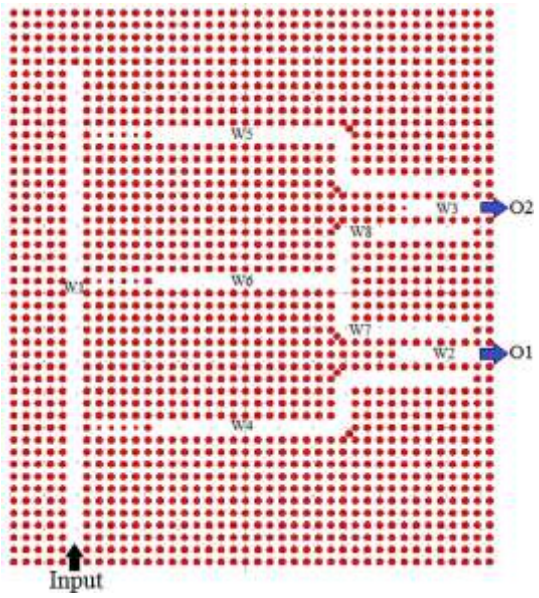

Fig.14 ADC with three nonlinear resonant cavities [91].

As Dariush et al. reported in [92], the OADC block consists of two cavity resonators. The structure is based on a = 434 nm, r = 0.3a and n= 3.49 with in GaAs substrate as shown in Fig.15. Using (Ph. Cs.) , and nonlinear properties to improve the speed of the structure around 1 TS/s that is much faster than the ADC in previous studies. The total footprint is equal to 42 μm^2. 2-D FDTD method was applied. The cavity and nonlinear properties led to gain low-power consumption and high-speed performance.

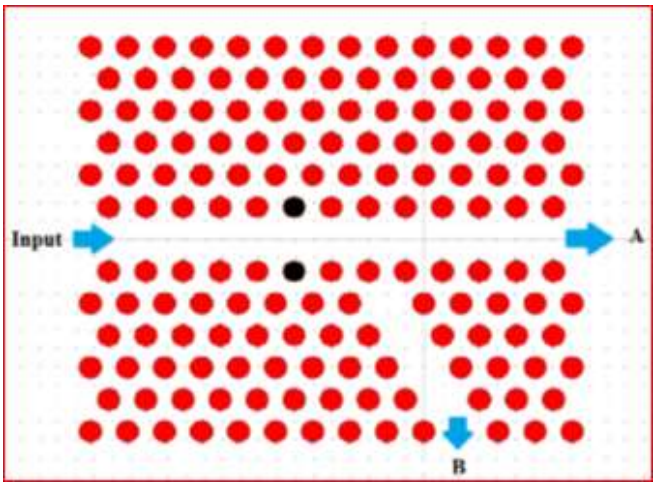

Fig.15 The structure ADC with two outputs [92].

The ADC has a maximum response time of around 4 ps and a sampling rate of 125 GS/s [93]. ADC is the most suitable device in photonic integrated circuits has minimum leakage loss and small footprint =1440 μm^2. As shown in Fig.16, the structure has r = 0.2a, n_0 = 1.4, $n_2 = 10^{-14}$ m^2/W and n= 3.46 surrounded by air. The PBG is 1214 <λ< 1821 nm in the wavelength range.

A Y-branch and three cavities resonators are used to implement 2-bits ADC [94]. The intensities of the optical input play a major role of the optical behavior so, it is important to shift the resonant mode of cavities to lower frequencies. A designed has n=3.46, r = 0.2a and a hexagonal lattice of silicon rods equal to 600 nm as shown in Fig.17. A large frequency band gap is equal to 1348 nm <λ< 2181 nm. The structure has the sampling rate and the total footprint equal to 253 μm^2 and 600 GS/s, respectively.

The results are getting better; the structure has a good sampling rate according to the previous structure. The best sampling rate is equal to 1000 GS/s which is the best result of all structures [92]. A brief comparison of all OADC will be collected in table 2. It includes the most remarkable properties for each cavity resonator design.

In the first structure in [91], the results are not good because the sampling rate is very small and has a large footprint. The structure of optical analog to digital converter in [92], has the best result because the structure has 1000 GS/s sampling rate and small area. In [94], the structure has good results too; the sampling rate is equal to 600 GS/s. The recent published paper in the same field can be found in [95]. It has a brief review about some structures exists in literature; but not states some novel trends that will be discussed in the next section.

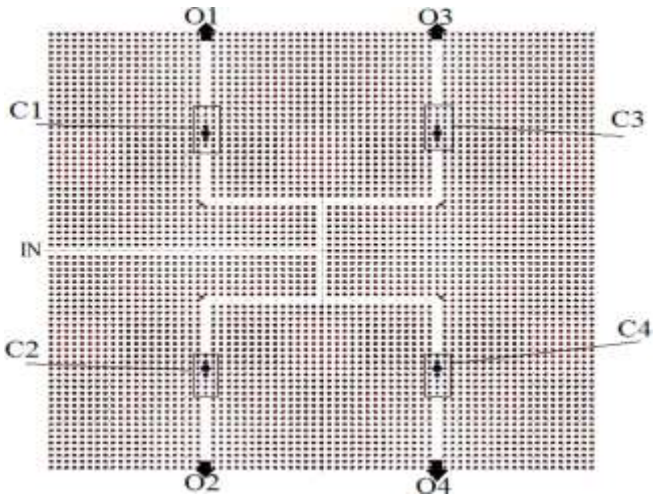

Fig.16 Optical circuit of ADC [93].

Fig.17 A Y-branch with three cavities resonators ADC [94].

VII. Challenges and Some Novel Trends

A. Challenges for the Design of Photonic Crystal Analog to Digital Converters

Challenges for the design of photonic crystal A/D converters may include the following points: -

a) The topological problem that means what the optimum topology that fits the required specifications.
b) The huge computer costs for simulating such devices.
c) What sort of optimizer that compromise between the computing cost and the required specifications?

TABLE 2 COMPARISONS BETWEEN THE PUBLISHED NONLINEAR CAVITY RESONATOR ADC IN THE LITERATURE

Years	[91, 2017]	[92, 2018]	[93, 2021]	[94, 2021]
Wavelength 1550 nm	1342 < λ <1611	1542< λ <1551	1214< λ <1821	1348< λ <2181
Footprint (μm^2)	924	42	1440	253
Lattice type	square	hexagonal	square	hexagonal
Lattice constant (a) nm	725	434	510	600
Refractive index	3.46	3.49	3.46	3.46
Linear refractive index	1.4	2.6	1.4	1.4
Nonlinear refractive index (m^2/W)	10^{-14}	$2.7x10^{-9}$	10^{-14}	0.01
Radius of the Si rod (nm)	0.26a	0.3a	0.2a	0.2a
Nonlinear rod material			nonlinear glass	doped glass
Input power range ($W/\mu m^2$)	0 -0.1	0 -0.21	0.06 - 0.24	0.1-0.35
Transfers (%)	80	NA	95	75
Sampling Rate (GS/s)	52	1000	125	600

B. Deep-learning for the Design of Photonic Crystal Analog to DigitalConverters

The ability of using the deep learning technique to design OADC will be studied. This technique will help us to choose the best parameters to be applied on the proposed structures of OADCs. We will get best results and save a lot of time compared with the traditional try and error techniques.

Deep learning method makes a computational mode that contains a lot of layers of processing units have the ability to learn multiple levels of abstraction information given in [96, 97]. The unique advantages of deep learning lie in its ability to analyze huge amount of data, and determine the useful needed information automatically based on historical background and key applications. At the near future deep learning will be essential in photonic design.

Using numerical simulation to optimize nanostructures with large number of possible combinations is computationally costly. For example, we may require long simulation time to compute electromagnetic field profile via (FDTD) methods to analyze the optical transmission response. It could take hours in the computing process, depending on the volume of photonic device [98].

In order to resolve this issue, we could use neural networks (NN) to implement an artificial intelligence integrated optimization process. NN can accelerate the optimization process by reducing the total number of the required simulations [99, 100].

VIII. CONCLUSION

In this paper, all OADCs are nonlinear applications based on Kerr effect in (Ph. Cs.). All types of OADC (1x2), (1x4) and (1x5) dimensions have been studied. The classification has been done based on the two techniques ring and cavity resonators of the proposed designs. A brief elaboration was established, and different remarkable characteristics were investigated. A cavity technique has the best results compared with ring resonators. It has small footprint and max sampling rate. By using the cavity technique, the structure of OADC in [92] has the best results because it has 1000 GS/s sampling rate and has a smallest area. In the ring resonator technique, the best results were at [82] because the sampling rate of OADC is 300 GS/s and its footprint are 240 μm^2.

All the structures were built on (2DPh.Cs.), the platform is arranged in an array of rods. The square and hexagonal lattice types have been used for the implementation process. The simulation and analysis are executed by using (PWE) and (FDTD) methods. This review combines the design and evaluating factors, thus bringing a good understanding of the proposed (OADC). In the future, ADC can be proposed with high performance by using deep learning technique.

REFERENCES

[1] R. Henderson, "Understanding optical fiber communications", Optics and Lasers in Engineering, vol. 38, no. 6, pp. 606-607, 2002. Available: 10.1016/s0143-8166(01)00181-6.
[2] R. Sinha and S. Rawal, "Modeling and design of 2D photonic crystal-based Y type dual band wavelength demultiplexer", Optical and Quantum Electronics, vol. 40, no. 9, pp. 603-613, 2008. Available: 10.1007/s11082-008-9248-z.
[3] V. Veselago, L. Braginsky, V. Shklover and C. Hafner, "Negative Refractive Index Materials", Journal of Computational and Theoretical

Nanoscience, vol. 3, no. 2, pp. 189-218, 2006. Available: 10.1166/jctn.2006.3000 [Accessed 23 November 2021].
[4] M. Richard De La Rue, Optical Properties of Photonic Structures, 1st ed. Boca Raton: CRC Press, 2012.
[5] S. McNab, N. Moll and Y. Vlasov, "Ultra-low loss photonic integrated circuit with membrane-type photonic crystal waveguides", Optics Express, vol. 11, no. 22, pp. 2927-2003. Available: 10.1364/oe.11.002927.
[6] G. Valley, "Photonic analog-to-digital converters", Optics Express, vol. 15, no. 5, pp. 1955-2007. Available: 10.1364/oe.15.001955.
[7] B. Miao, C. Chen, A. Sharkway, S. Shi and D. Prather, "Two-bit optical analog-to-digital converter based on photonic crystals", Optics Express, vol. 14, no. 17, pp. 7966-2006. Available: 10.1364/oe.14.007966.
[8] M. Xiong et al., "All-optical 10 Gb/s AND logic gate in a silicon microring resonator", Optics Express, vol. 21, no. 22, pp. 25772-2013. Available: 10.1364/oe.21.025772.
[9] M. Moradi, M. Danaie and A. Orouji, "Design of all-optical XOR and XNOR logic gates based on Fano resonance in plasmonic ring resonators", Optical and Quantum Electronics, vol. 51, no. 5,pp. 1-18, 2019. Available: 10.1007/s11082-019-1874-0.
[10] H. Alipour-Banaei, M. Jahanara and F. Mehdizadeh, "T-shaped channel drop filter based on photonic crystal ring resonator", Optik, vol. 125, no. 18, pp. 5348-5351, 2014. Available: 10.1016/j.ijleo.2014.06.056.
[11] L. Li and G. Liu, "Photonic crystal ring resonator channel drop filter", Optik - International Journal for Light and Electron Optics, vol. 124, no. 17, pp. 2966-2968, 2013. Available: 10.1016/j.ijleo.2012.09.012.
[12] A. Dideban, H. Habibiyan and H. Ghafoorifard, "Photonic crystal channel drop filters based on fractal structures", Physica E: Low-dimensional Systems and Nanostructures, vol. 63, pp. 304-310, 2014. Available: 10.1016/j.physe.2014.06.009.
[13] Y. Wang, D. Chen, G. Zhang, J. Wang and S. Tao, "A super narrow band filter based on silicon 2D photonic crystal resonator and reflectors", Optics Communications, vol. 363, pp. 13-20, 2016. Available: 10.1016/j.optcom.2015.10.070." Opt. Commun. 363, 13–20 (2016).
[14] H. Alipour-Banaei and F. Mehdizadeh, "Significant role of photonic crystal resonant cavities in WDM and DWDM communication tunable filters", Optik - International Journal for Light and Electron Optics, vol. 124, no. 17, pp. 2639-2644, 2013. Available: 10.1016/j.ijleo.2012.07.029.," Optik124, 2639–2644 (2013).
[15] M. Djavid and M. Abrishamian, "Multi-channel drop filters using photonic crystal ring resonators", Optik, vol. 123, no. 2, pp. 167-170, 2012. Available: 10.1016/j.ijleo.2011.04.001.," Optik123, 167–170 (2012).
[16] M. Djavid, A. Ghaffari, F. Monifi and M. Abrishamian, "T-shaped channel-drop filters using photonic crystal ring resonators", Physica E: Low-dimensional Systems and Nanostructures, vol. 40, no. 10, pp. 3151-3154, 2008. Available: 10.1016/j.physe.2008.05.002.
[17] C. Ren, P. Wang, L. Cheng, S. Feng, L. Gan and Z. Li, "Multichannel W3 Y-branch filter in a two dimensional triangular-lattice photonic crystal slab", Optik, vol. 125, no. 24, pp. 7203-7206, 2014. Available: 10.1016/j.ijleo.2014.07.139.
[18] S. Rezaee, M. Zavvari and H. Alipour-Banaei, "A novel optical filter based on H-shape photonic crystal ring resonators", Optik, vol. 126, no. 20, pp. 2535-2538, 2015. Available: 10.1016/j.ijleo.2015.06.043.
[19] S. Roshan Entezar, "Photonic crystal wedge as a tunable multichannel filter", Superlattices and Microstructures, vol. 82, pp. 33-39, 2015. Available: 10.1016/j.spmi.2015.01.039.
[20] M. Rakhshani and M. Mansouri-Birjandi, "Realization of tunable optical filter by photonic crystal ring resonators", Optik, vol. 124, no. 22, pp. 5377-5380, 2013. Available: 10.1016/j.ijleo.2013.03.114.
[21] M. Youcef Mahmoud, G. Bassou and F. Metehri, "Channel drop filter using photonic crystal ring resonators for CWDM communication systems", Optik, vol. 125, no. 17, pp. 4718-4721, 2014. Available: 10.1016/j.ijleo.2014.04.084.
[22] M. Youcef Mahmoud, G. Bassou, A. Taalbi and Z. Chekroun, "Optical channel drop filters based on photonic crystal ring resonators", Optics Communications, vol. 285, no. 3, pp. 368-372, 2012. Available: 10.1016/j.optcom.2011.09.068.
[23] A. Taalbi, G. Bassou and M. Youcef Mahmoud, "New design of channel drop filters based on photonic crystal ring resonators", Optik, vol. 124, no. 9, pp. 824-827, 2013. Available: 10.1016/j.ijleo.2012.01.045.
[24] M. Reza Rakhshani and M. Ali Mansouri-Birjandi, "Design and simulation of wavelength demultiplexer based on heterostructure photonic crystals ring resonators", Physica E: Low-dimensional Systems and Nanostructures, vol. 50, pp. 97-101, 2013. Available: 10.1016/j.physe.2013.03.003.
[25]A. Khorshidahmad and A. Kirk, "Composite superprism photonic crystal demultiplexer: analysis and design", *Optics Express*, vol. 18, no. 19, pp. 20518-20528,2010. Available: 10.1364/oe.18.020518.
[26] F. Mehdizadeh, M. Soroosh and H. Alipour-Banaei, "An optical demultiplexer based on photonic crystal ring resonators", Optik, vol. 127, no. 20, pp. 8706-8709, 2016. Available: 10.1016/j.ijleo.2016.06.086.
[27] A. Rostami, H. Banaei, F. Nazari and A. Bahrami, "An ultra-compact photonic crystal wavelength division demultiplexer using resonance cavities in a modified Y-branch structure", Optik, vol. 122, no. 16, pp. 1481-1485, 2011. Available: 10.1016/j.ijleo.2010.05.036.
[28] H. Alipour-Banaei, F. Mehdizadeh and M. Hassangholizadeh-Kashtiban, "A novel proposal for all optical PhC-based demultiplexers suitable for DWDM applications", Optical and Quantum Electronics, vol. 45, no. 10, pp. 1063-1075, 2013. Available: 10.1007/s11082-013-9717-x.
[29] D. Bernier, X. Le Roux, A. Lupu, D. Marris-Morini, L. Vivien and E. Cassan, "Compact, low cross-talk CWDM demultiplexer using photonic crystal superprism", Optics Express, vol. 16, no. 22, pp. 17209-17214, 2008. Available: 10.1364/oe.16.017209.
[30] X. Zhang, Q. Liao, T. Yu, N. Liu and Y. Huang, "Novel ultracompact wavelength division demultiplexer based on photonic band gap", Optics Communications, vol. 285, no. 3, pp. 274-276, 2012. Available: 10.1016/j.optcom.2011.10.001.
[31] M. Mansouri-Birjandi and M. Rakhshani, "A new design of tunable four-port wavelength demultiplexer by photonic crystal ring resonators", Optik, vol. 124, no. 23, pp. 5923-5926, 2013. Available: 10.1016/j.ijleo.2013.04.128.
[32] I. Ouahab and R. Naoum, "A novel all optical 4×2 encoder switch based on photonic crystal ring resonators", Optik, vol. 127, no. 19, pp. 7835-7841, 2016. Available: 10.1016/j.ijleo.2016.05.080.
[33] A. Sharkawy, S. Shi, D. Prather and R. Soref, "Electro-optical switching using coupled photonic crystal waveguides", Optics Express, vol. 10, no. 20, pp. 1048-2002. Available: 10.1364/oe.10.001048.
[34] Y. Zhang, Y. Zhang and B. Li, "Optical switches and logic gates based on self-collimated beams in two-dimensional photonic crystals", Optics Express, vol. 15, no. 15, pp. 9287-2007. Available: 10.1364/oe.15.009287.
[35] N. Mohammed, "Performance Evaluation and Enhancement of 2×2 Ti: LiNbO3 Mach Zehnder Interferometer Switch at 1.3 μm and 1.55 μm", *The Open Electrical & Electronic Engineering Journal*, vol. 6, no. 1, pp. 36-49, 2012. Available: 10.2174/1874129001206010036 [Accessed 28 February 2022].
[36] S. Serajmohammadi, H. Alipour-Banaei and F. Mehdizadeh, "All optical decoder switch based on photonic crystal ring resonators", Optical and Quantum Electronics, vol. 47, no. 5, pp. 1109-1115, 2014. Available: 10.1007/s11082-014-9967-2.
[37] T. Mostafa, N. Mohammed and E. El-Rabaie, "Ultra-High bit rate all-optical AND/OR logic gates based on photonic crystal with multi-wavelength simultaneous operation", Journal of Modern Optics, vol. 66, no. 9, pp. 1005-1016, 2019. Available: 10.1080/09500340.2019.1598587.
[38] T. Moniem, "All optical active high decoder using integrated 2D square lattice photonic crystals", Journal of Modern Optics, vol. 62, no. 19, pp. 1643-1649, 2015. Available: 10.1080/09500340.2015.1061061.
[39] H. Alipour-Banaei, F. Mehdizadeh, S. Serajmohammadi and M. Hassangholizadeh-Kashtiban, "A 2*4 all optical decoder switch based on photonic crystal ring resonators", Journal of Modern Optics, vol. 62, no. 6, pp. 430-434, 2014. Available: 10.1080/09500340.2014.957743.
[40] M. Ghadrdan and M. Mansouri-Birjandi, "Concurrent implementation of all-optical half-adder and AND& XOR logic gates based on nonlinear photonic crystal", Optical and Quantum Electronics, vol. 45, no. 10, pp. 1027-1036, 2013. Available: 10.1007/s11082-013-9713-1.
[41] W. Liu, D. Yang, G. Shen, H. Tian and Y. Ji, "Design of ultra-compact all-optical XOR, XNOR, NAND and OR gates using photonic crystal multi-mode interference waveguides", Optics & Laser Technology, vol. 50, pp. 55-64, 2013. Available: 10.1016/j.optlastec.2012.12.030.
[42] N. Saidani, W. Belhadj and F. AbdelMalek, "Novel all-optical logic gates based photonic crystal waveguide using self-imaging phenomena", Optical and Quantum Electronics, vol. 47, no. 7, pp. 1829-1846, 2014. Available: 10.1007/s11082-014-0047-4.
[43] A. Salmanpour, S. Mohammadnejad and P. Omran, "All-optical photonic crystal NOT and OR logic gates using nonlinear Kerr effect and ring resonators", Optical and Quantum Electronics, vol. 47, no. 12, pp. 3689-3703, 2015. Available: 10.1007/s11082-015-0238-7.
[44] P. Rani, Y. Kalra and R. Sinha, "Design and analysis of polarization independent all-optical logic gates in silicon-on-insulator photonic crystal", Optics Communications, vol. 374, pp. 148-155, 2016. Available: 10.1016/j.optcom.2016.04.037.
[45] H. Alipour-Banaei, S. Serajmohammadi and F. Mehdizadeh, "All optical NOR and NAND gate based on nonlinear photonic crystal ring resonators", Optik, vol. 125, no. 19, pp. 5701-5704, 2014. Available: 10.1016/j.ijleo.2014.06.013.

[46] M. Shehata and N. Mohammed, "Design and optimization of novel two inputs optical logic gates (NOT, AND, OR and NOR) based on single commercial TW-SOA operating at 40 Gbit/s", *Optical and Quantum Electronics*, vol. 48, no. 6, pp. 336-352, 2016. Available: 10.1007/s11082-016-0602-2 [Accessed 28 February 2022].
[47] T. Moniem, "All-optical digital 4 × 2 encoder based on 2D photonic crystal ring resonators", Journal of Modern Optics, vol. 63, no. 8, pp. 735-741, 2015. Available: 10.1080/09500340.2015.1094580.
[48] R. Jannesari, C. Ranacher, C. Consani, T. Grille and B. Jakoby, "Sensitivity optimization of a photonic crystal ring resonator for gas sensing applications", Sensors and Actuators A: Physical, vol. 264, pp. 347-351, 2017. Available: 10.1016/j.sna.2017.08.017.
[49] D. Vigneswaran, N. Ayyanar, M. Sharma, M. Sumathi, M. M.S. and K. Porsezian, "Salinity sensor using photonic crystal fiber", Sensors and Actuators A: Physical, vol. 269, pp. 22-28, 2018. Available: 10.1016/j.sna.2017.10.052 [Accessed 23 November 2021].
[50] A. Bahabady, S. Olyaee and H. Arman, "Optical Biochemical Sensor Using Photonic Crystal Nano-ring Resonators for the Detection of Protein Concentration", Current Nanoscience, vol. 13, no. 4, pp.421-425, 2017. Available: 10.2174/1573413713666170405161211.
[51] S. Kim et al., "Two-dimensional photonic crystal hexagonal waveguide ring laser", Applied Physics Letters, vol. 81, no. 14, pp. 2499-2501, 2002. Available: 10.1063/1.1510583.
[52] F. Sohrabi, T. Mahinroosta and S. Hamidi, "Design of 1 × 3 power splitter based on photonic crystal ring resonator", Optical Engineering, vol. 53, no. 11, pp. 115104-2014. Available: 10.1117/1.oe.53.11.115104.
[53] Y. Yang, K. Lin, I. Yang, K. Lee, W. Lee and Y. Tsai, "All-optical photonic-crystal encoder capable of operating at multiple wavelengths", Optik, vol. 142, pp. 354-359, 2017. Available: 10.1016/j.ijleo.2017.05.067.
[54] T. Mostafa and E. El-Rabaie, "Literature Review on All-Optical Photonic Crystal Encoders and Some Novel Trends", Menoufia Journal of Electronic Engineering Research, vol. 28, no. 2, pp. 153-184, 2019. Available: 10.21608/mjeer.2019.62773.
[55] G. Calo and V. Petruzzelli, "Wavelength Routers for Optical Networks-on-Chip Using Optimized Photonic Crystal Ring Resonators", IEEE Photonics Journal, vol. 5, no. 3, pp. 7901011-7901011, 2013. Available: 10.1109/jphot.2013.2264278.
[56] J. Lu et al., "Wavelength routers with low crosstalk using photonic crystal point defect micro-cavities", Optik, vol. 127, no. 6, pp. 3235-3242, 2016. Available: 10.1016/j.ijleo.2015.11.235.
[57] M. Bottacini, F. Poli, A. Cucinotta and S. Selleri, "Modeling of Photonic Crystal Fiber Raman Amplifiers", Journal of Lightwave Technology, vol. 22, no. 7, pp. 1707-1713, 2004. Available: 10.1109/jlt.2004.831087.
[58]J. Limpert et al., "Low-nonlinearity single-transverse-mode ytterbium-doped photonic crystal fiber amplifier", Optics Express, vol. 12, no. 7, pp. 1313-1319, 2004. Available: 10.1364/opex.12.001313.
[59] C. Wu, C. Liu and Z. Ouyang, "Compact and low-power optical logic NOT gate based on photonic crystal waveguides without optical amplifiers and nonlinear materials", Applied Optics, vol. 51, no. 5,pp. 680-685, 2012. Available: 10.1364/ao.51.000680.
[60] C. Robin, I. Dajani and B. Pulford, "Modal instability-suppressing, single-frequency photonic crystal fiber amplifier with 811 W output power", Optics Letters, vol. 39, no. 3,pp.666-669, 2014. Available: 10.1364/ol.39.000666.
[61] A. Cucinotta, F. Poli and S. Selleri, "Design of Erbium-Doped Triangular Photonic-Crystal-Fiber-Based Amplifiers", IEEE Photonics Technology Letters, vol. 16, no. 9, pp. 2027-2029, 2004. Available: 10.1109/lpt.2004.833109.
[62] H. Gibbs, S. McCall and T. Venkatesan, "Optical Bistable Devices: The Basic Components of All-Optical Systems?", Optical Engineering, vol. 19, no. 4, pp. 75-80, 1980. Available: 10.1117/12.7972544.
[63] S. Smith, "Optical bistability, photonic logic, and optical computation", Applied Optics, vol. 25, no. 10, pp. 1550-1564, 1986. Available: 10.1364/ao.25.001550.
[64] S. Jensen, "The Nonlinear Coherent Coupler", IEEE Transactions on Microwave Theory and Techniques, vol. 30, no. 10, pp. 1568-1571, 1982. Available: 10.1109/tmtt.1982.1131291.
[65] K. Leung and Y. Liu, "Photon band structures: The plane-wave method", Physical Review B, vol. 41, no. 14, pp. 10188-10190, 1990. Available: 10.1103/physrevb.41.10188.
[66] A. Salimzadeh and H. Alipour-Banaei, "An all optical 8 to 3 encoders based on photonic crystal OR-gate ring resonators", Optics Communications, vol. 410, pp. 793-798, 2018. Available: 10.1016/j.optcom.2017.11.036.
[67] A. Dyogtyev, I. Sukhoivanov and R. De La Rue, "Photonic band-gap maps for different two dimensionally periodic photonic crystal structures", Journal of Applied Physics, vol. 107, no. 1, pp. 13108-13114, 2010. Available: 10.1063/1.3247544.
[68] K. Ho, C. Chan and C. Soukoulis, "Existence of a photonic gap in periodic dielectric structures", Physical Review Letters, vol. 65, no. 25, pp. 3152-3155, 1990. Available: 10.1103/physrevlett.65.3152.
[69] R. Luebbers and K. Kunz, "Finite difference time domain calculations of antenna mutual coupling", IEEE Transactions on Electromagnetic Compatibility, vol. 34, no. 3, pp. 357-359, 1992. Available: 10.1109/15.155855.
[70] M. Rycroft, "Computational electrodynamics, the finite-difference time-domain method", Journal of Atmospheric and Terrestrial Physics, vol. 58, no. 15, pp. 1817-1818, 1996. Available: 10.1016/0021-9169(96)80449-1.
[71] P. Rani, Y. Kalra and R. Sinha, "Realization of AND gate in Y shaped photonic crystal waveguide", Optics Communications, vol. 298-299, pp. 227-231, 2013. Available: 10.1016/j.optcom.2013.02.014.
[72] R. Younis, N. Areed and S. Obayya, "Fully Integrated AND and OR Optical Logic Gates", IEEE Photonics Technology Letters, vol. 26, no. 19, pp. 1900-1903, 2014. Available: 10.1109/lpt.2014.2340435.
[73] F. Mehdizadeh, M. Soroosh and H. Alipour-Banaei, "Proposal for 4-to-2 optical encoder based on photonic crystals", IET Optoelectronics, vol. 11, no. 1, pp. 29-35, 2017. Available: 10.1049/iet-opt.2016.0022.
[74] A. Rostami and G. Rostami, "Full optical analog to digital (A/D) converter based on Kerr-like nonlinear ring resonator", Optics Communications, vol. 228, no. 1-3, pp. 39-48, 2003. Available: 10.1016/j.optcom.2003.09.085.
[75] B. Youssefi, M. K. Moravvej-Farshi, and N. Granpayeh, "Two-bit all-optical analog-to-digital converter based on nonlinear Kerr effect in 2D photonic crystals," Opt. Commun., vol. 285, no. 13–14, pp. 3228–3233, Jun. 2012.
[76] A. Rostami and G. Rostami, "Full optical analog to digital (A/D) converter based on Kerr-like nonlinear ring resonator", Optics Communications, vol. 228, no. 1-3, pp. 39-48, 2003. Available: 10.1016/j.optcom.2003.09.085 [Accessed 22 June 2022].
[77] H. Saghaei, V. Heidari, M. Ebnali-Heidari and M. Yazdani, "A systematic study of linear and nonlinear properties of photonic crystal fibers", Optik, vol. 127, no. 24, pp. 11938-11947, 2016. Available: 10.1016/j.ijleo.2016.09.111.
[78] F. Mehdizadeh, M. Soroosh, H. Alipour-Banaei and E. Farshidi, "A Novel Proposal for All Optical Analog-to-Digital Converter Based on Photonic Crystal Structures", IEEE Photonics Journal, vol. 9, no. 2, pp. 1-11, 2017. Available: 10.1109/jphot.2017.2690362.
[79] F. Mehdizadeh, M. Soroosh, H. Alipour-Banaei and E. Farshidi, "Ultra-fast analog-to-digital converter based on a nonlinear triplexer and an optical coder with a photonic crystal structure", Applied Optics, vol. 56, no. 7, pp. 1799-2017. Available: 10.1364/ao.56.001799.
[80] M. Sani, S. Khosroabadi and A. Shokouhmand, "A novel design for 2-bit optical analog to digital (A/D) converter based on nonlinear ring resonators in the photonic crystal structure", Optics Communications, vol. 458, pp. 124760-124783, 2020. Available: 10.1016/j.optcom.2019.124760.
[81] X. Geng and L. Zhao, "All-optical analog to digital converter based on nonlinear photonic crystal ring resonators", Photonics and Nanostructures - Fundamentals and Applications, vol. 41,pp. 100817-100838, 2020. Available: 10.1016/j.photonics.2020.100817.
[82] S. Khosroabadi, A. Shokouhmand and S. Marjani, "Full optical 2-bit analog to digital convertor based on nonlinear material and ring resonators in photonic crystal structure", Optik, vol. 200, pp.163393-163399, 2020. Available: 10.1016/j.ijleo.2019.163393.
[83] A. Shamsi and R. Moradi, "All optical analog to digital convertor using nonlinear photonic crystal ring resonators", Optical and Quantum Electronics, vol. 52, no. 10, pp. 435-447, 2020. Available: 10.1007/s11082-020-02541-z.
[84] S. Naghizade and H. Saghaei, "An ultra-fast optical analog-to-digital converter using nonlinear X-shaped photonic crystal ring resonators", Optical and Quantum Electronics, vol. 53, no. 3, pp. 149-164, 2021. Available: 10.1007/s11082-021-02798-y.
[85]B. Shoop, Photonic Analog-to-Digital Conversion, 1st ed. Berlin, Heidelberg: Springer Berlin Heidelberg, 2001.
[86]A. Rostami and G. Rostami, "Full optical analog to digital (A/D) converter based on Kerr-like nonlinear ring resonator", Optics Communications, vol. 228, no. 1-3, pp. 39-48, 2003. Available: 10.1016/j.optcom.2003.09.085.
[87] G. Rostami and A. Rostami, "All-optical integrated coding system for optical analog to digital (A/D) converter", Laser Physics Letters, vol. 1, no. 8, pp. 406-410, 2004. Available: 10.1002/lapl.200410091.

[88] A. Tavousi, M. Mansouri-Birjandi and M. Saffari, "Successive approximation-like 4-bit full-optical analog-to-digital converter based on Kerr-like nonlinear photonic crystal ring resonators", Physica E: Low-dimensional Systems and Nanostructures, vol. 83, pp. 101-106, 2016. Available: 10.1016/j.physe.2016.04.007.
[89] A. Tavousi and M. Mansouri-Birjandi, "Optical-analog-to-digital conversion based on successive-like approximations in octagonal-shape photonic crystal ring resonators", Superlattices and Microstructures, vol. 114, pp. 23-31, 2018. Available: 10.1016/j.spmi.2017.11.021.
[90] J. Chen, F. Mehdizadeh, M. Soroosh and H. Alipour-Banaei, "A proposal for 5-bit all optical analog to digital converter using nonlinear photonic crystal-based ring resonators", Optical and Quantum Electronics, vol. 53, no. 9, pp.510-518, 2021. Available: 10.1007/s11082-021-03166-6.
[91] F. Mehdizadeh, M. Soroosh, H. Alipour-Banaei and E. Farshidi, "All optical 2-bit analog to digital converter using photonic crystal-based cavities", Optical and Quantum Electronics, vol. 49, no. 1,pp. 38-48, 2017. Available: 10.1007/s11082-016-0880-8.
[92] D. Jafari, T. Nurmohammadi, M. Asadi and K. Abbasian, "All-optical analog-to-digital converter based on Kerr effect in photonic crystal", Optics & Laser Technology, vol. 101, pp. 138-143, 2018. Available: 10.1016/j.optlastec.2017.11.007.
[93] S. RamtinFard, M. Salehi and E. Abiri, "Ultra-fast all-optical ADC using nonlinear ring resonators in photonic crystal microstructure", Optical and Quantum Electronics, vol. 53, no. 2, pp. 120-133, 2021. Available: 10.1007/s11082-021-02769-3.
[94] M. Aghaei and A. Bahrami, "An optical analog-to-digital converter based on nonlinear resonant cavities in photonic crystals", Optical and Quantum Electronics, vol. 53, no. 5, pp.233-244, 2021. Available: 10.1007/s11082-021-02880-5.
[95] M. Mohammadi, F. Habibi, M. Seifouri, and S. Olyaee, “Recent advances on all-optical photonic crystal analog-to-digital converter (ADC),” Opt. Quantum Electron., vol. 54, no. 3, pp. 1-11, 2022. Available: 10.1007/s11082-022-03568-0.
[96] Y. LeCun, Y. Bengio and G. Hinton, "Deep learning", Nature, vol. 521, no. 7553, pp. 436-444, 2015. Available: 10.1038/nature14539.
[97] A. Krizhevsky, I. Sutskever and G. Hinton, "ImageNet classification with deep convolutional neural networks", Communications of the ACM, vol. 60, no. 6, pp. 84-90, 2017. Available: 10.1145/3065386 [Accessed 21 June 2022].
[98] M. Tahersima et al., "Deep Neural Network Inverse Design of Integrated Photonic Power Splitters", *Scientific Reports*, vol. 9, no. 1, pp. 1368-1376, 2019. Available: 10.1038/s41598-018-37952-2.
[99] K. Kojima, B. Wang, U. Kamilov, T. Koike-Akino and K. Parsons, "Acceleration of FDTD-based Inverse Design Using a Neural Network Approach", Advanced Photonics 2017 (IPR, NOMA, Sensors, Networks, SPPCom, PS), 2017. Available: 10.1364/iprsn.2017.itu1a.4 [Accessed 21 June 2022].
[100] M. Teng, K. Kojima, T. Koike-Akino, B. Wang, C. Lin and K. Parsons, "Broadband SOI mode order converter based on topology optimization", Optical Fiber Communication *Co*nference, 2018. Available: 10.1364/ofc.2018.th2a.8 [Accessed 21 June 2022].